A comparative study of leg geometry for energy-efficient locomotion

Pranav A. Bhounsule[a], Jason Pusey[b], Chelsea Moussouni[a]

***Abstract*— It has been theorized that biological legs or the serial leg with a knee and hip joint has evolved over centuries for energy efficient locomotion and as such, has been adapted into a multitude of legged robots. However, recent success of legged robots with alternate leg morphologies without actuated knees, such as the parallel and symmetric five-bar link leg raises the question: which leg geometry is more energy-efficient and why? To answer this question, we created a minimal model of bipedal walking whose non-dimensionalised equations of motion have a single free parameter, the leg ratio and defined as the ratio of the distal to the proximal leg length. Then we performed an energy minimization for a given leg ratio and combination of speed and step length. When we optimized mechanical work, we found that all three legs have an identical efficiency, but the symmetric leg has the lowest peak torque. When we optimized a cost representative of an electric motor, we found that the serial leg is most energy efficient for all leg ratios, and the cost decreases as the leg ratio increases. For a leg ratio of 1, the parallel and symmetric leg have identical efficiencies. As the leg ratio increases, the efficiency of the symmetric leg approaches that of the serial leg while that of parallel leg decreases. However, the symmetric leg produces the least peak torque followed by the serial leg for leg ratios greater than 1. Our conclusion is that the symmetric leg rivals the serial leg by being easier to design and having smaller peak torques leading to smaller actuators at the cost of being slightly less energy-efficient.**

I. Introduction

Creating energy-efficient dynamic legged systems is one of the outstanding challenges in the area of legged robotics. This depends on factors such as the type and number of actuators, the mass distribution or the passive dynamics of the robot, the presence or lack of springs in the leg and their arrangement (e.g., serial, parallel), the leg morphology, the presence or lack of a foot and its design (e.g., passive, active), and the control policy. A fundamental understanding of the role of each of these factors on the energy efficiency is key in creation of legged robots that are economical in terms of energy usage.

In this paper, we focus on the role of leg morphology in the energetics of legged locomotion. The most commonly used leg design is biological limb or the serial leg (see Fig. 2 a) with a thigh and a shank and actuated at the hip and knee joints. However, roboticists have used non-anthropomorphic leg designs such as the prismatic leg (see Fig. 1 a), the parallel five-bar leg, and the symmetric five-bar leg (see Fig. 2 b and c). There has been no research that has compared the various leg designs for energy efficiency in an objective way. Such a study has the potential of helping make better leg design choices for energy-efficient locomotion.

We provide a practical way of comparing the different leg designs using a minimal model of walking and using trajectory optimization. The minimal model consists of a point mass body and a telescopic leg. We use Jacobian from the joint space to the foot space to relate the telescopic leg to the leg geometry of interest. After we non-dimensionalise the equations, we have a single free parameter which we call the leg ratio, r, defined as the ratio of the distal (e.g., shank) to the proximal (e.g., thigh) link length. We use trajectory optimization to search for the most energy-efficient gait for a given r and combination of step length, D, and step velocity, V. We look at two cost functions; first based on mechanical work, and second based on electric motor model. Exhaustive numerical searches are carried to identify trends in energy efficiency for the different leg designs and for different leg ratios. This work is expected to provide an objective way of comparing different leg geometries for energy-efficiency which will guide not only leg design but also the selection of actuators.

II. Background and Related Work

We first review the different leg architectures emphasizing the critical aspects of design and actuation and then present past attempts at comparing them.

The serial leg geometry (see Fig. 2 a), which resembles the biological leg, is the design of choice for most legged robots, and consists of an actuated hip and knee. The simplest design choice is to place the knee actuator at the joint (e.g., Darwin OP [1]) but adds to the weight of the leg and increases the energy cost of leg swing. An alternate choice is to place the knee actuator at the hip and use a transmission (e.g., cables [2]) to drive the knee joint, but this makes the design more complex.

The design complications of the serial leg have lead to the parallel five-bar leg used on ATRIAS [3] (see Fig. 2 b), the symmetric five-bar linkage used on UPenn Minitaur [4] and MIT Super Mini Cheetah [5] (see Fig. 2 c). Because both the actuators are at the hip, this allows for the legs to be light weight. The actuators in these two designs also share the load at the foot.

Keneally et al. [4] have compared the serial, parallel five-bar, and the symmetric five-bar leg with respect to their ability to sense forces at the joints, ability for force production, and thermal cost of producing a force. They found that the symmetric five-bar leg is superior than the other two geometries for these three metrics. Abate et al.

[a] Dept. of Mechanical Engineering, University of Texas San Antonio, One UTSA Circle, San Antonio, TX 78249, USA. Corresponding author: pranav.bhounsule@utsa.edu. [b] Army Research Laboratory, Aberdeen Proving Grounds, Aberdeen, MD 210001, UTSA. PAB and CM were supported by NSF grant IIS 1566463 and PAB was also supported by UTSA, Office of the Vice President for Research.

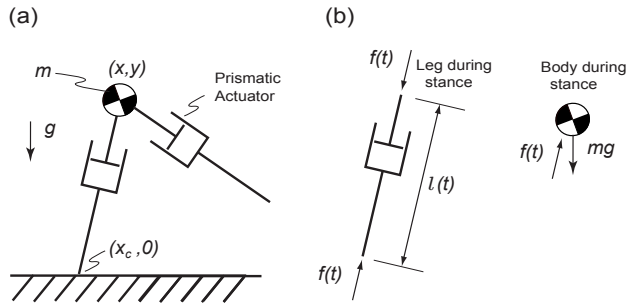

Fig. 1. (a) The minimal bipedal model. (b) Free body diagram for the minimal model in stance phase.

[6] compared the serial and the parallel five-bar with respect to energy efficiency. In their simulation study, they imposed a ground reaction force profile and body trajectory obtained from human running experiments and then used optimization to compute joint torques, speeds, and consequently the mechanical cost of transport, MCOT (a energy metric, see Eqn. 4). They found that the serial leg has lower MCOT and lower peak torque then the parallel five-bar leg. Our study is different from this study in that we do not impose any predefined trajectory or forces but allow the optimization to freely choose the trajectory, forces, torques, speeds to minimize an energy-based cost function. Further, we non dimensionalize the equations of motion revealing that there is a single free parameter for each leg, thus enabling easy comparison between the three leg geometries.

III. Methods

A. Minimal biped model

The minimal bipedal model is shown in Fig. 1 (a) [7] consists of two massless legs connected to each other at a point mass body with mass m. Each of the legs have a prismatic actuator that can apply a compressive leg force, $f(t)$, that will cause the leg length to vary as a function of time, $l(t)$. Gravity, g, points downwards as shown. Since the legs are massless they can change their length and orientation instantaneously and without an energetic cost between steps. However, when the legs are on the ground they have to work to move the point mass body, and there is an associated energetic cost.

The free body diagram for the point mass in stance phase is shown in Fig. 1 (b). We assume that only one foot can be in contact with the ground at any point of time. Thus, during stance phase, the point mass body is acted upon by the actuator force and gravity. Further, we assume that the left and right legs have identical motion, thus it is sufficient to simulate a single step. Throughout this paper, we seek periodic motions such that the current step is the same as the previous step.

The equations of motion can be written as follows:

$$m\ddot{x} = f\frac{x - x_c}{\ell}, \qquad m\ddot{y} = f\frac{y}{\ell} - mg, \tag{1}$$

where x and y are the x- and y- position of the body, x_c is the contact point of the leg during stance phase, and the leg length, $\ell = \sqrt{(x - x_c)^2 + y^2}$.

To simplify the formulation of the optimization problem we set $x_c = 0$ and rewrite the equations in non-dimensional form as follows:

$$\ddot{X} = F\frac{X}{\sqrt{X^2 + Y^2}}, \qquad \ddot{Y} = F\frac{Y}{\sqrt{X^2 + Y^2}} - 1, \tag{2}$$

where the non-dimensional parameters are defined as follows:

$$F = \frac{f}{mg} \qquad X = \frac{x}{\ell_{max}} \qquad Y = \frac{y}{\ell_{max}}$$
$$\dot{X} = \frac{\dot{x}}{\sqrt{g\ell_{max}}} \qquad \dot{Y} = \frac{\dot{y}}{\sqrt{g\ell_{max}}},$$

and ℓ_{max} is the maximum leg length.

B. Optimization problem

The optimization problem is to find initial conditions $X(0) = X_0$, $Y(0) = Y_0$, $\dot{X}(0) = \dot{X}_0$, $\dot{Y}(0) = \dot{Y}_0$, and non-dimensional leg force $F(t)$ to minimize the Cost Of Transport (COT) defined as:

$$\text{COT} = \frac{\text{Energy Used}}{\text{Weight} \times \text{Distance Travelled}}. \tag{3}$$

The constraints are that periodicity requires $X(T) = X_0 + D$, $Y(T) = Y_0$, $\dot{X}(T) = \dot{X}_0$, and $\dot{Y}(T) = \dot{Y}_0$, where non-dimensional step time, T, and step length, D, are specified in advance. Thus, the step velocity, V, can be obtained by the relation $D = VT$. The leg length constraint is such that throughout stance phase, $L_{min} \leqslant \sqrt{X^2 + Y^2} \leqslant L_{max}$. The values for these are defined in Sec. III-C. The ground reaction force constraint is $0 \leqslant F \leqslant 3$; that is, the ground reaction force can be up to 3 times the weight of the robot. We use a nonlinear constraint parameter optimization software, SNOPT [8]. Also, we discretize the ground reaction force, $F(t)$ as a piecewise linear function of time over a grid of size $N + 1$ (a user chosen value). That is the grid points are $0 = \tau_0, \tau_1, \tau_2, ..., \tau_N = T$ and $\tau_i - \tau_{i-1} = T/N$ $(i = 0, 1, ...N)$, and the corresponding $N + 1$ forces at grid points are $F_0, F_1, F_2, ..., F_N$.

We consider two cost functions. The first one uses the absolute value of the mechanical work done ($\int |T\omega| dt$) and is called the Mechanical Cost Of Transport (MCOT):

$$\text{MCOT} = \frac{1}{D}\int_0^T |\mathbf{\Gamma}^T(\tau)\dot{\mathbf{\Theta}}(\tau)| d\tau, \tag{4}$$

where the degrees of freedom for the legs (see Sec. III-C for details) are $\mathbf{\Theta} = [\theta_1,\ \theta_2]$, and non-dimensional actuator torques are $\mathbf{\Gamma} = [\Gamma_1,\ \Gamma_2]$. The torques are non-dimensionalised by $mg\ell_{max}$. The absolute value of a continuous variable has a kink or a discontinuous first derivative at 0. Since we use a smooth optimization program that relies on smooth gradients, the optimization will have numerical difficulties close to 0. So, we smooth the absolute value using arctan smoothing described in Srinivasan [9] (pp. 62).

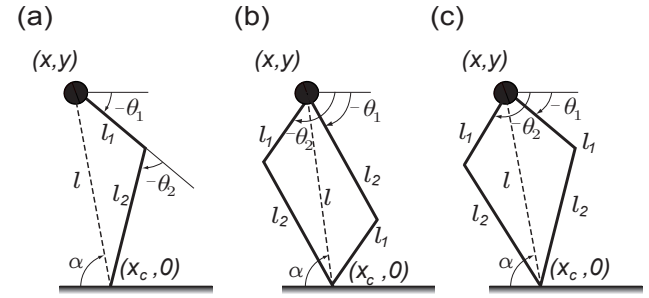

Fig. 2. Various leg geometries that have demonstrated energy-efficient locomotion: (a) serial leg, (b) parallel five-bar leg, and (c) symmetric five-bar leg. Note that for (b) and (c), there is a bar connecting the two motors placed at the body joint and is the fifth link.

The second one is representative of energy used in electric motors ($\int T^2 dt$) [1] and called the Total Cost Of Transport (TCOT):

$$\text{TCOT} = \frac{1}{D}\int_0^T \mathbf{\Gamma}(\tau)^T \mathbf{\Gamma}(\tau) d\tau. \tag{5}$$

Also, to get actual TCOT for a specific motor, one needs to multiply the TCOT by R/K^2 where R is the resistance of the windings and K is the motor constant.

In summary, the optimization problem is solved as follows. The equations of motion and the cost function are integrated from one grid point to another using the integrator DOP853 [10] with a tolerance of 10^{-12}. After integrating over a complete step, one can evaluate the constraint violation in the periodicity and the leg length constraint at the grid points. The optimization software varies the parameters, $X_0, Y_0, \dot{X}_0, \dot{Y}_0, F_{i=0,1,\ldots N}$, so as to meet the constraints within 10^{-6} while reducing the cost function. We also map the linear prismatic leg length, $\ell(\tau)$, and leg force, $F(\tau)$, for a particular leg in order to compute the actuator angles, $\dot{\mathbf{\Theta}}(\tau)$, and actuator torques, $\mathbf{\Gamma}(\tau)$. This is discussed next.

C. Leg geometries

We consider three leg geometries as shown in Fig. 2, each of which have different torques, $\mathbf{\Gamma}$. The serial leg geometry in (a) is the biological leg and has one actuated joint at the hip (shown as θ_1) and the other at the knee (shown as θ_2) and needs substantial energy for leg swing because the hip actuator needs to drive the mass of the knee actuator. The parallel five-bar mechanism in (b) is asymmetric about the vertical line and is used on Oregon State ATRIAS [3], a bipedal robot. This design has both actuators at the hip which reduces the leg mass. Finally, the symmetric five-bar leg is used on the quadruped robots, UPenn Minitaur [4] and MIT Super Mini Cheetah [5], and like the parallel leg, has the advantage of having both the actuators at the hip, thus reducing the leg mass.

First, we present the computation of the Jacobian of the forward kinematics for the three leg geometries. The foot position, $g_x(q)$ (where $q = (\theta_1, \theta_2)$ and $x = O$ for open (serial) leg, $x = P$ for parallel five-bar leg, and $x = S$ for symmetric five-bar leg, relative to the body at (x, y) for the three leg geometries is given by [4]:

$$g_O(q) = \mathbf{R}(\theta_1)\begin{bmatrix}\ell_1 + \ell_2\cos\theta_2 \\ \ell_2 \sin\theta_2\end{bmatrix}, \tag{6}$$

$$g_P(q) = \mathbf{R}(\alpha_1)\Big(\ell_2\mathbf{R}(\alpha_2) + \ell_1\mathbf{R}^T(\alpha_2)\Big)\begin{bmatrix}1\\0\end{bmatrix}, \tag{7}$$

$$g_S(q) = \mathbf{R}(\alpha_1)\begin{bmatrix}\ell_1\cos\alpha_2 + \sqrt{\ell_2^2 - \ell_1^2\sin^2\alpha_2} \\ 0\end{bmatrix}, \tag{8}$$

$$\mathbf{R}(\theta) = \begin{bmatrix}\cos\theta & -\sin\theta \\ \sin\theta & \cos\theta\end{bmatrix}, \tag{9}$$

$$\alpha_1 = 0.5(\theta_1 + \theta_2) \text{ and } \alpha_2 = 0.5(\theta_1 - \theta_2) \tag{10}$$

The above expressions can be used to derive the Jacobian of the forward kinematics, $J = D_q g(q)$.

Second, we show how to relate the virtual leg parameters, the leg length ℓ and the landing angle α (see Fig. 2), to the actuator degrees of freedom, q.

$$\text{Open (Serial): } \theta_1 = \alpha - 0.5\pi + \phi_{\ell_2} \tag{11}$$

$$\theta_2 = \pi + \phi_\ell \tag{12}$$

$$\text{Parallel: } \alpha_1 = \alpha - 0.5(\pi - \phi_{\ell_2} - \phi_{\ell_1}) \tag{13}$$

$$\alpha_2 = 0.5(\phi_{\ell_1} + \phi_{\ell_2}) \tag{14}$$

$$\text{Symmetric: } \alpha_1 = \alpha - 0.5\pi \tag{15}$$

$$\alpha_2 = \phi_{\ell_2} \tag{16}$$

$$\text{where } \phi_\ell = \cos^{-1}\left(\frac{\ell_1^2 + \ell_2^2 - \ell^2}{2\ell_1\ell_2}\right) \tag{17}$$

$$\phi_{\ell_1} = \cos^{-1}\left(\frac{\ell^2 + \ell_2^2 - \ell_1^2}{2\ell_2\ell}\right) \tag{18}$$

$$\phi_{\ell_2} = \cos^{-1}\left(\frac{\ell^2 + \ell_1^2 - \ell_2^2}{2\ell_1\ell}\right) \tag{19}$$

During the course of optimization there is the possibility that evaluation of $\cos^{-1}$ will lead to an imaginary number when the argument is greater than 1. To prevent this from happening we smoothen the function $\cos^{-1}$ using the technique mentioned in Srinivasan [11] (see supplement, pp. 5).

Finally, we show how to compute the torque, $\mathbf{\Gamma}$. To do so, we use virtual work which states that

$$\mathbf{F}^T\dot{\ell} = \mathbf{\Gamma}^T\dot{\mathbf{\Theta}}, \tag{20}$$

where $\mathbf{F}$, ℓ are vectors that hold the x- and y-component of the ground reaction forces and leg length respectively. But we know that

$$\dot{\ell} = \mathbf{J}\dot{\mathbf{\Theta}} \tag{21}$$

We put Eqn. 21 into Eqn. 20 to get

$$\mathbf{\Gamma} = \mathbf{J}^T\mathbf{F} \tag{22}$$

To summarize, given the leg length, ℓ, and landing angle, α, we compute q using Eqns. 11 - 16 and then use Eqns. 6-10 to compute the Jacobian, J. Finally, we find the torque,

[1]The energy used in the motors is the sum of dissipative losses in the windings (T^2) and mechanical work done ($T\omega$). However, the dissipative losses dominates the mechanical work

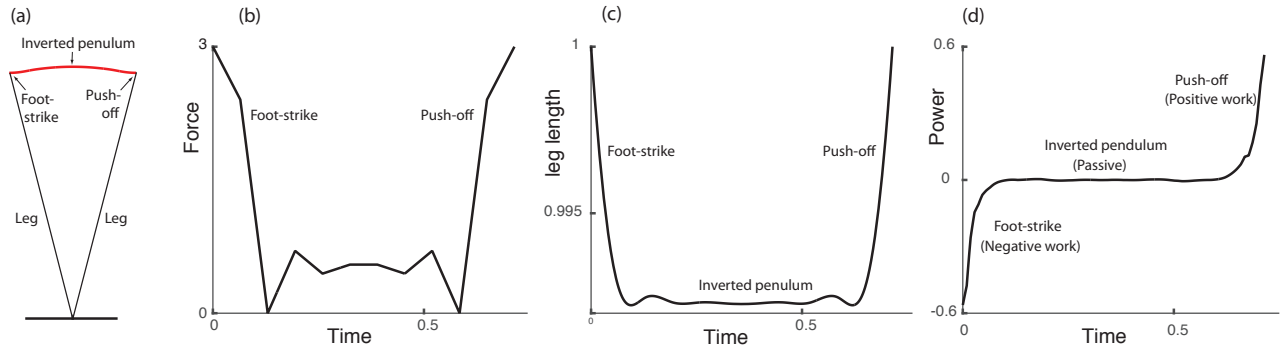

Fig. 3. Results for MCOT minimization: (a) Center of mass trajectory, (b) Ground reaction force, (c) Virtual Leg length, and (d) Mechanical power.

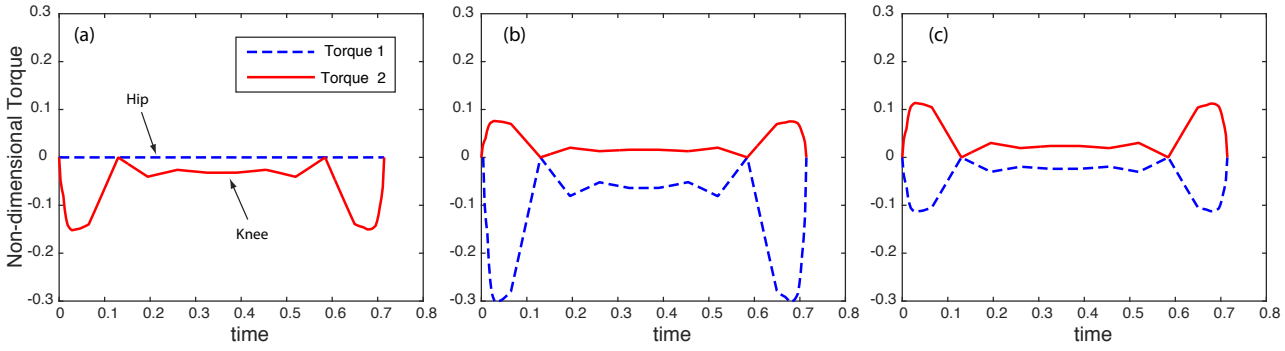

Fig. 4. Results for minimization of MCOT. Torque for (a) serial, (b) parallel, and (c) symmetric leg for $r = 2$, $V = 0.7$, and $D = 0.5$.

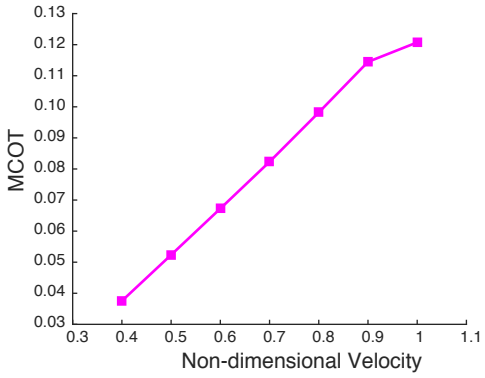

Fig. 5. MCOT versus non-dimensional velocity. The MCOT is independent of the leg configuration.

$\mathbf{\Gamma}$, from the Jacobian, $\mathbf{J}$, and ground reaction force $\mathbf{F}$ using Eqn. 22.

IV. Results

A. Minimizing mechanical work ($\int |T\omega| dt$)

We minimized the absolute value of the mechanical work per unit weight per unit distance moved, i.e., MCOT (see Eqn. 4) for a given leg, a leg ratio, r (defined as $\ell_2 = r\ell_1$), and a combination of speed, V, and step length, D. We found that the MCOT is the same for all leg geometries and independent of leg ratio, r. This is not surprising because the mechanical work done by the joints is the same as the mechanical work done by the ground reaction force in lengthening/shortening the prismatic leg due to the principal of virtual work (see Eqn. 20). Further, Fig. 5 shows a plot of MCOT as a function of V for a fixed $D = 0.5$ and $r = 2$. MCOT increases linearly with the speed, indicating that the mechanical work increases as the speed increases.

Next we take a closer look at the optimization results for the combination, $V = 0.7$ and $D = 0.5$. The MCOT $= 0.0823$. The trajectory of the body, mass m, is shown in Fig. 3 (a) and resembles an inverted pendulum. The force profile, leg length, and mechanical power (force times change in leg length) is shown in Fig. 3 (b), (c), and (d) respectively. At the beginning, there is a negative force with shortening of the leg which corresponds to negative power. This corresponds to a foot-strike. Thereafter, the force and leg length remains constants which leads to zero power. At the end, the force increases with lengthening of the leg which corresponds to positive power. This indicates a push-off.

Finally to get a sense of magnitude of torques at the actuators, we compute the joint torques using the ground reaction force and Jacobian (see Sec. III-C) for leg ratio, $r = 2$. The results for each leg are shown in Fig. 4. For the serial leg in (a), the hip motor is passive (zero work) while the knee motor is applying an active torque to shorten the leg during foot-strike and lengthen the leg during push-off.

However, in the case of parallel leg in (b) and symmetric leg in (c), both motors are doing the work. In the parallel leg, the two motors apply unequal force while the motor torques are equal and opposite for the symmetric leg. Although all these geometries do the same mechanical work, the peak torques are lowest in the symmetric leg. The serial and parallel leg have peak torques of 1.5 and 3 times that of the symmetric leg respectively.

B. Minimizing motors costs ($\int T^2 dt$)

We minimized the electric losses per unit weight per unit distance moved, i.e., TCOT (see Eqn. 5) for a given leg, leg ratio, r, and combination of speed, V, and step length, D. Unlike MCOT minimization, we found that the TCOT is different for different legs and leg ratios. The Fig. 7 (a), (b), and (c) shows a plot of the TCOT as a function of speed, V, for a fixed step length, $D = 0.5$. Each plot is for a different leg ratio, r, and has three curves corresponding to the three leg configurations. At $r = 1$, the symmetric leg and the parallel leg are identical and have the same costs (the two curves line up on top of each other as shown in Fig. 7 (a)). The serial leg however has the lowest cost and is between a factor of 2.5 to 3.5 over the symmetric and parallel legs. At $r = 2$, the symmetric leg becomes more energy-efficient than the parallel leg, and it comes closer to the serial leg. The symmetric and serial leg are about a factor of 4 and 6 better than the parallel leg respectively. Finally, at $r = 4$, the symmetric is slightly less energy-efficient then the serial leg, but about a factor 30 better than the parallel leg. Note that as r increases, the symmetric leg become more energy-efficient and approaches the serial leg as $r \to \infty$. At $r = \infty$ or $\ell_1 = 0$, both legs have same energy-efficiencies. Also, we found that as r increases, the energy efficiency improves for the symmetric and serial legs and becomes worse for the parallel leg. This is explained in the next paragraph.

Next, we take a closer look at the energy-optimal solution for $r = 2$ and the combination $V = 0.7$ and $D = 0.5$ for the three leg geometries to understand why one leg is more energy-efficient than the other. We found that although the energetics and torque profiles are different, the trajectory, ground reaction forces, and leg length are a function of time and mostly identical. We show plots in Fig. 6 but only for the serial leg geometry at $r = 2$. It is interesting to note that the motion resembles an inverted pendulum and looks qualitatively similar to the MCOT minimization results shown in Fig. 3. However, the TCOT's for the three legs are different. The TCOT for the serial leg, parallel leg, and symmetric leg are 0.0049, 0.0293, and 0.0073 (units $\Omega A^2/Nm$) respectively. Thus, the serial leg is about two times more energy-efficient than the symmetric leg and about 4 times more energy-efficient than the parallel leg configuration at the specific V, D combination. To understand the vastly different costs, we look at a plot of torque and power as a function of time. From Fig. 8 (a) and (c), we observe that the peak torques for the serial leg and the symmetric leg are almost the same. However, the the hip actuator is passive while only the knee actuator is doing the work. But in case of the symmetric leg, since both actuators are doing the work, the cost is about twice that of a serial leg. Finally, the parallel leg, because of the asymmetry, uses different torques at the two motors. The peak torque on one actuator is about two times the serial or the symmetric leg, and this causes the power to be almost four times as large, because the power (T^2) scales with peak torque.

V. Discussion

We have compared three commonly used bipedal leg morphologies—serial, parallel five-bar, and symmetric five-bar—for walking energetics. We used a minimal model of locomotion and formulated an optimization problem to minimize an energy-based cost function subject to various kinematic and actuator bounds. Specifically, we considered two cost functions, mechanical work ($T\omega$) and electrical dissipation costs (T^2), associated with an electric motor. We found that for the mechanical work minimization, all leg geometries give identical costs, but the peak torque in the symmetric leg is the lowest followed by that of the serial leg, and finally that of the parallel leg. We also found that for the electric motor cost minimization, the serial leg is most energy-efficient, and the parallel leg is least energy efficient. The symmetric leg has the same efficiency as that of the parallel leg at $r = 1$, and it approaches the efficiency of the serial leg as $r \to \infty$ (see Fig 7). Finally, we found that all leg morphologies at all leg ratios we considered and for both the cost functions give qualitatively similar motions: a quick dissipative foot-strike followed by inverted pendulum-like motion for a majority of the stance phase, and ending with a quick push-off during support exchange.

The fact that the biological (serial) leg is the most energy-efficient geometry is interesting, because it lends credence to the theory that evolution chooses the best design [12]. Further, we note that for the serial leg at $V = 0.7$, $D = 0.5$ and $r = 1$, the TCOT (all in units of $\Omega A^2/Nm$) is about 6×10^{-3} but decreases to 5×10^{-3} at $r = 2$ and to 4×10^{-3} at $r = 4$. Thus, the energy efficiency increases as r increases, so $r = 1$ gives the least energy-efficient design. But, human leg has $r \approx 1$ [13]. This might be because of a design tradeoff between energy efficiency and other evolution pressures. For example, at $r = 1$, when the thigh and shank are of equal length, the major muscles on these joints can be about equal size to allow for optimal performance on other tasks such as jumping.

The serial leg morphology is very common in most legged robots including bipeds, quadruped, and humanoid robots, perhaps because it is a more anthropomorphic design. Note that the serial leg needs an actuated knee. However, adding an actuator to the knee requires the hip motor to drive this added weight during swing phase thus increasing the energetic costs. One way to circumvent this is to place the actuator at the hip and drive the knee through suitable transmission (e.g., MIT Cheetah [14], [15]). But constructing the serial leg in this configuration may limit the range of motion and exploration of this topic is beyond the scope of this paper. On the other hand, the parallel and five-bar links have their

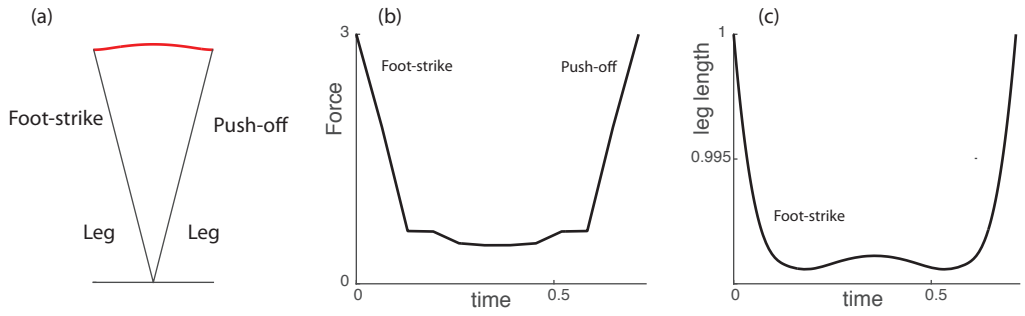

Fig. 6. Results for TCOT minimization for $r = 2$ for serial leg: (a) body trajectory, (b) ground reaction force, and (c) virtual leg length. The symmetric and parallel legs optimizations give similar plots.

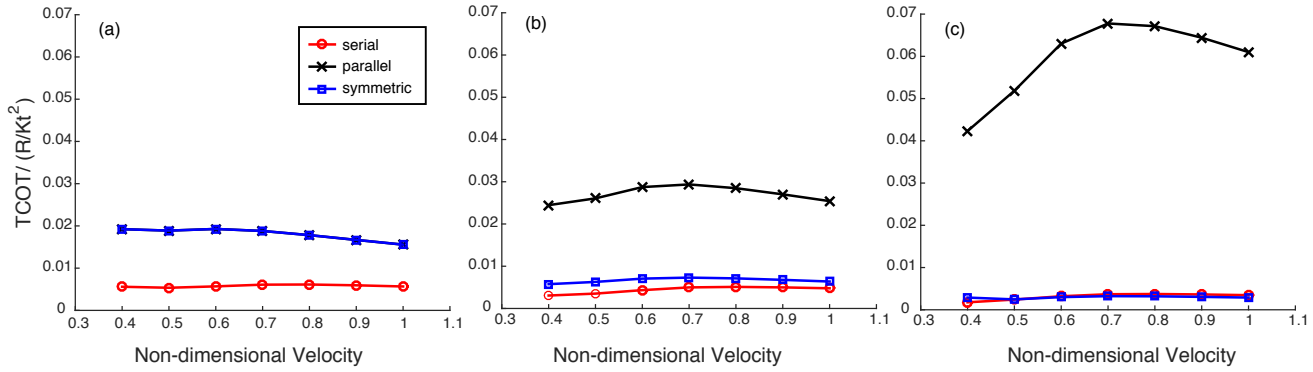

Fig. 7. TCOT versus non-dimensional velocity for different leg geometries. Each plots corresponds a specific leg ratio r, where $\ell_2 = r\ell_1$. (a) $r = 1$, (b) $r = 2$, and (c) $r = 4$.

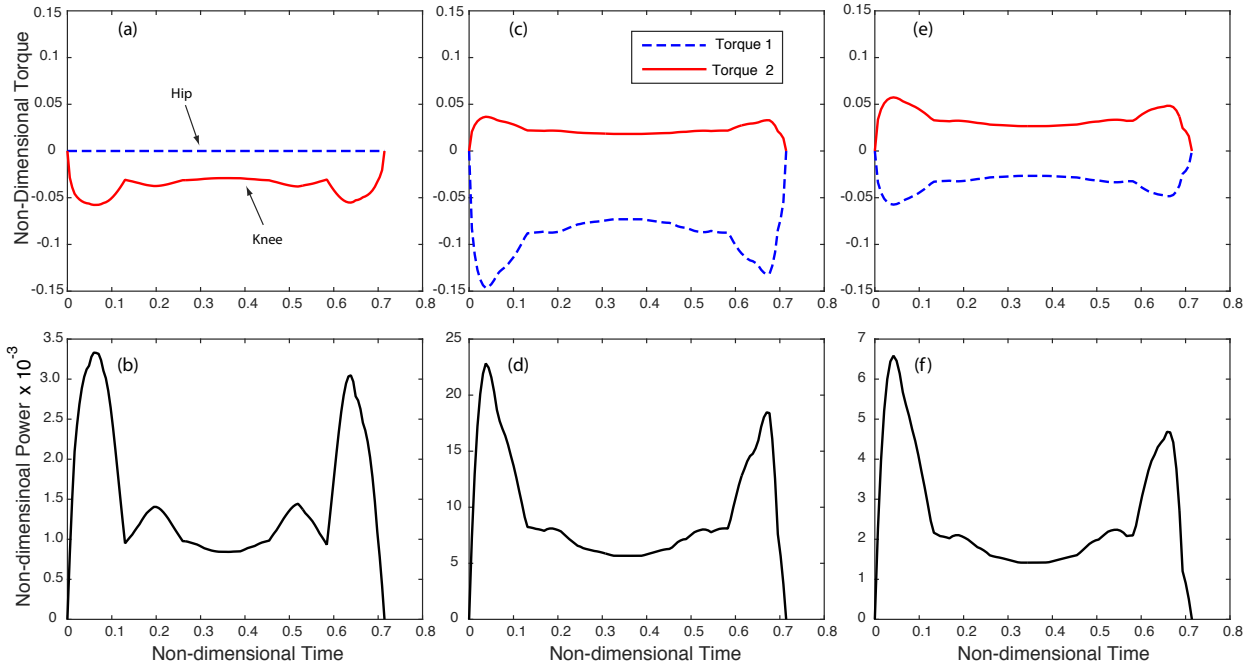

Fig. 8. Results for TCOT minimization at $V = 0.7$, $D = 0.5$ for $r = 2$. Top row shows Torque versus time and bottom row shows Power versus time. Specifically, (a,b) serial leg, (c,d) parallel leg, and (e,f) symmetric leg.

actuators at the hip, enabling lightweight legs yet simple leg design.

The peak torque is the least for the symmetric leg, followed by that of the serial leg for the same leg ratio and combination of step length and speed (see Figs. 4 and 8). This has implications in the choice of the actuator: the symmetric leg needs relatively smaller actuators then the other two designs.

A surprising result was that all three leg geometries for the two costs we considered produced identical body trajectories: a foot-strike followed by an (almost) inverted pendulum-like motion, and ending in push-off before the next foot-strike. A considerable number of past work has focussed on using the linear inverted pendulum model [16] to create walking motion. This model requires the body to maintain a constant height above the ground, and thus it requires a bent knee. This is clearly less energy-efficient compared to the inverted pendulum model discovered in the optimization here, because it creates an essentially passive motion through a large part of the gait. Another interesting result is that the energy-optimal gait discovered requires the leg to be at its singular configuration at foot-strike and push-off, a position that is avoided most times, as it can lead to infinite torques due to singular Jacobian.

Our work has limitations which we highlight next. We have ignored the cost of swinging the leg, which can be non-trivial if the legs have mass. The parallel bar linkage, though least efficient in our analysis, can perhaps be made more efficient by adding a toe (as done in ATRIAS). We have only looked at energy-optimal bipedal walking motions. Further work on running gaits and for quadrupeds needs to be undertaken to generalize these results. Thus, eventually, a more detailed robot model with a toe and a swing leg, and for various running gaits and for multi-legged robots will provide a complete picture on how energy-efficiency depends on the leg morphology.

REFERENCES

[1] I. Ha, Y. Tamura, H. Asama, J. Han, and D. W. Hong, "Development of open humanoid platform darwin-op," in *SICE Annual Conference (SICE), 2011 Proceedings of*. IEEE, 2011, pp. 2178–2181.

[2] J. P. Schmiedeler and K. J. Waldron, "Leg stiffness and articulated leg design for dynamic locomotion," in *ASME 2002 International Design Engineering Technical Conferences and Computers and Information in Engineering Conference*. American Society of Mechanical Engineers, 2002, pp. 1105–1112.

[3] J. A. Grimes and J. W. Hurst, "The design of atrias 1.0 a unique monopod, hopping robot," in *Proceedings of the 2012 International Conference on Climbing and Walking Robots and the Support Technologies for Mobile Machines*, 2012, pp. 548–554.

[4] G. Kenneally, A. De, and D. Koditschek, "Design principles for a family of direct-drive legged robots," *IEEE Robotics and Automation Letters*, vol. 1, no. 2, pp. 900–907, 2016.

[5] W. Bosworth, S. Kim, and N. Hogan, "The mit super mini cheetah: A small, low-cost quadrupedal robot for dynamic locomotion," in *2015 IEEE International Symposium on Safety, Security, and Rescue Robotics (SSRR)*. IEEE, 2015, pp. 1–8.

[6] A. Abate, J. W. Hurst, and R. L. Hatton, "Mechanical antagonism in legged robots," in *Robotics Science and Systems (RSS)*, 2016.

[7] M. Srinivasan and A. Ruina, "Computer optimization of a minimal biped model discovers walking and running," *Nature*, vol. 439, no. 7072, pp. 72–75, 2005.

[8] P. Gill, W. Murray, and M. Saunders, "SNOPT: An SQP algorithm for large-scale constrained optimization," *SIAM Journal on Optimization*, vol. 12, no. 4, pp. 979–1006, 2002.

[9] M. Srinivasan, "Why walk and run: energetic costs and energetic optimality in simple mechanics-based models of a bipedal animal," Ph.D. dissertation, Cornell University, 2006.

[10] E. Hairer, S. P. Nrsett, and G. Wanner, *Solving Ordinary Differential Equations: Nonstiff problems. v. 2: Stiff and differential-algebraic problems*. Springer Verlag, 2010.

[11] M. Srinivasan, "Fifteen observations on the structure of energy-minimizing gaits in many simple biped models," *Journal of The Royal Society Interface*, vol. 8, no. 54, pp. 74–99, 2011.

[12] R. M. Alexander, *Optima for animals*. Princeton University Press, 1996.

[13] R. Huston, *Principles of biomechanics*. CRC press, 2008.

[14] A. Ananthanarayanan, M. Azadi, and S. Kim, "Towards a bio-inspired leg design for high-speed running," *Bioinspiration & biomimetics*, vol. 7, no. 4, p. 046005, 2012.

[15] S. Seok, A. Wang, M. Y. Chuah, D. Otten, J. Lang, and S. Kim, "Design principles for highly efficient quadrupeds and implementation on the mit cheetah robot," in *Robotics and Automation (ICRA), 2013 IEEE International Conference on*. IEEE, 2013, pp. 3307–3312.

[16] S. Kajita, F. Kanehiro, K. Kaneko, K. Yokoi, and H. Hirukawa, "The 3d linear inverted pendulum mode: A simple modeling for a biped walking pattern generation," in *International Conference on Intelligent Robots and Systems, Hawaii, USA*, 2001, pp. 239–246.